JOURNAL OF THEORETICAL
AND APPLIED MECHANICS
1, **39**, 2001

AN IMPROVED NUMERICAL APPROACH FOR INVERSE SIMULATIONS OF AIRCRAFT MANOEUVRES

GRZEGORZ KOWALECZKO

Military University of Technology, Warsaw
e-mail: kowaleczko@wul.wat.waw.pl

Method of spatial manoeuvres modelling based on solving the inverse problem of dynamics is presented in this paper. A detailed description of the inverse problem solution is shown. To illustrate the method, results of numerical simulations for two selected manoeuvres are also included.

Key words: inverse simulation, flight dynamics

Notations

For an aeroplane:

- $\boldsymbol{X}$ – vector of flight parameters $\boldsymbol{X} = [V, \alpha, \beta, P, Q, R, \Theta, \Phi, \Psi, x_g, y_g, z_g]$
- V – velocity of flight
- α, β – angle of attack, sideslip angle, respectively
- P, Q, R – angular velocity components (body axes)
- Θ, Φ, Ψ – Euler angles of fuselage
- x_g, y_g, z_g – position coordinates
- $\boldsymbol{S}$ – vector of control parameters, $\boldsymbol{S} = [T_c, \delta_H, \delta_L, \delta_V]$
- T_c – thrust of engines
- $\delta_H, \delta_L, \delta_V$ – deflections of stabilator, aileron and rudder, respectively

For a helicopter:

- $\boldsymbol{X}$ – vector of flight parameters $\boldsymbol{X} = [U, V, W, P, Q, R, \Theta, \Phi, \Psi, x_g, y_g, z_g, \omega]$
- U, V, W – linear velocity components (body axes)
- ω – angular velocity of the main rotor
- $\boldsymbol{S}$ – vector of control parameters, $\boldsymbol{S} = [\theta_0, \kappa_s, \eta_s, \phi_{tr}]$

θ_0 – main rotor collective pitch angle
κ_s, η_s – longitudinal and lateral cyclic pitch angles
ϕ_{tr} – tail rotor collective pitch angle

1. Introduction

An inverse problem is and has always been one of the main problems of classical mechanics (Galiullin, 1986). At present, inverse methods are used to determine active forces acting on a mechanical system, parameters of this system and limits put on the system corresponding to a given motion. The fundamental task in inverse simulation applied to flight dynamics is determination of the control inputs (displacements of control surfaces and thrust of the engine) that are necessary to perform the required spatial manoeuvre.

There are various methods of solution which can be applied to these problems. Sometimes the methods based on the solution of sets of differential-algebraic equations are applied (Blajer, 1994a,b; Blajer and Parczewski, 1987, 1991). These methods require certain complicated transformations and the final form of differential-algebraic equations directly depends on the assumed constraints of motion of the object. Methods of decomposition of the control task are also applied (Tomczyk, 1996). However, these methods are based on the assumption that relations between the forces and moments acting on the object and that the controls are linear.

In this paper, a special numerical method of solution of the inverse problem is applied. It is based on linearization of the considered problem around a current position of the object in the state space. The main advantage of this method is that it doesn't need any transformation of equations of the object motion. Equations are the same as in classical problems of the object motion (object motion with determined control signals). There are no limits imposed on the relations between forces and controls. This method has been applied with success to dynamic flight problems of aeroplanes and helicopters (Thomson and Bradley, 1990; Hess et al., 1991; Hess and Gao, 1993; Rutherford and Thomson, 1996a,b).

2. Mathematical model of objects

The inverse simulation has been applied to reconstruct certain aircraft ma-

noeuvres. Manoeuvres of a helicopter and an aeroplane have been considered. Both objects have been treated as rigid bodies with six degrees of freedom. In both cases, their dynamics is described by sets of nonlinear differential equations. They can be symbolically written in the form

$$\mathbf{A}(t, \boldsymbol{X})\frac{d\boldsymbol{X}}{dt} + \boldsymbol{B}(t, \boldsymbol{X}) = \boldsymbol{F}(t, \boldsymbol{X}, \boldsymbol{S}) \tag{2.1}$$

Vector $\boldsymbol{X} \in \mathcal{R}^{n_x}$ is the vector of flight parameters and $\boldsymbol{S} \in \mathcal{R}^{n_s}$ is the vector of control parameters.

For a helicopter, additionally, dynamics of a blade flapping motion has been taken into account. In this case, the set (2.1) should be complemented by the following set of nonlinear algebraic equations

$$\widehat{\mathbf{L}}(\boldsymbol{X}, \boldsymbol{S}, \boldsymbol{\beta})\boldsymbol{\beta} = \boldsymbol{F}(\boldsymbol{X}, \boldsymbol{S}, \boldsymbol{\beta}) \tag{2.2}$$

where $\boldsymbol{\beta} = [a_0, a_1, b_1]$ is a vector determining orientation of the cone of the main rotor in relation to the fuselage.

3. Inverse simulation algorithm

The set (2.1) is transformed to the following form

$$\frac{d\boldsymbol{X}}{dt} = \dot{\boldsymbol{X}} = \boldsymbol{G}(t, \boldsymbol{X}, \boldsymbol{S}) \tag{3.1}$$

which could be integrated using one of the numerical methods (for instance the Runge-Kutta method).

Vector $\boldsymbol{G}$ is equal to

$$\boldsymbol{G} = \mathbf{A}^{-1}(\boldsymbol{F} - \boldsymbol{B}) \tag{3.2}$$

The output vector $\boldsymbol{Y} \in \mathcal{R}^{n_y}$ is uniquely determined by the vector of flight parameters $\boldsymbol{X}$

$$\boldsymbol{Y} = \boldsymbol{D}(\boldsymbol{X}) \tag{3.3}$$

In the present considerations both vectors are the same

$$\boldsymbol{Y} = \boldsymbol{X} \tag{3.4}$$

The set (3.1) is completed by the following initial conditions

$$\boldsymbol{X}(t_0) = \boldsymbol{X}_0 \tag{3.5}$$

As it was mentioned, in the considered case, the fundamental problem is to determine the control vector $\boldsymbol{S}(t)$ for the defined output vector $\boldsymbol{Y}_z(t)$, which describes constraints of the object motion.

The problem is made discrete for successive time points $t_0, ..., t_k, t_{k+1}, ..., t_N$. For each instant t_{k+1}, the vector $\boldsymbol{Y}_z(t_{k+1})$ is defined by constraints of the motion. The vector $\boldsymbol{X}(t_{k+1})$ is also calculated as a result of integration of the set (3.1) in the time interval from t_k to t_{k+1}. This interval is determined in the way which preserves the stability of final solution. Because the described procedure requires one constant time step and because of a nonlinearity of the problem, this step is determined by numerical experiments. This means that several simulations should be performed with decreasing time intervals up to the moment when two convergent solutions are obtained. The method is in agreement with the Runge-Kutta method with different time interval. The time interval is dependent upon every individual problem. According to (3.1), because the derivative $d\boldsymbol{X}/dt$ depends on the control vector $\boldsymbol{S}(t_k)$, the calculated value $\boldsymbol{X}(t_k)$ also depends on this control vector. The vector $\boldsymbol{Y}(t_{k+1})$ determined on the basis of relation (3.3) has to be equal to the specified value $\boldsymbol{Y}_z(t_{k+1})$. Difference between the calculated value of the vector $\boldsymbol{Y}(t_{k+1})$ and the constrained vector $\boldsymbol{Y}_z(t_{k+1})$ is the basis for the calculation of a corrected value of the control vector $\boldsymbol{S}(t_k)$.

This procedure has an iterative character. It means that for each time point t_k, a finite number of iterations is performed till the assumed compatibility between vectors $\boldsymbol{Y}$ and $\boldsymbol{Y}_z$ is obtained. In the ith iteration, the following operations are performed:

- On the basis of known values of $\boldsymbol{X}(t_k)$ and $\boldsymbol{S}^{(m)}(t_k)$, making use of (3.1), the derivative is calculated

$$\dot{\boldsymbol{X}}^{(m)}(t_k) = \boldsymbol{G}[t_k, \boldsymbol{X}(t_k), \boldsymbol{S}^{(m)}(t_k)] \tag{3.6}$$

- The value of flight parameters and output vector at the time point t_{k+1} is determined by numerical integration of relation (3.6)

$$\begin{aligned} \boldsymbol{X}^{(m)}(t_{k+1}) &= \boldsymbol{X}(t_k) + \int_{t_k}^{t_{k+1}} \dot{\boldsymbol{X}}^{(m)}(t_k)\, dt \\ \boldsymbol{Y}^{(m)}(t_{k+1}) &= \boldsymbol{D}[\boldsymbol{X}^{(m)}(t_{k+1})] \end{aligned} \tag{3.7}$$

- The difference between the defined output vector $\boldsymbol{Y}_z(t_{k+1})$ and the vector calculated from (3.7) is determined

$$\Delta\boldsymbol{Y}^{(m)}(t_{k+1}) = \boldsymbol{Y}_z(t_{k+1}) - \boldsymbol{Y}^{(m)}(t_{k+1}) \tag{3.8}$$

If this difference is smaller than the defined accuracy $\varepsilon_{\boldsymbol{Y}}$, calculations are continued at the next time point t_{k+2}. The vector of flight parameters and the control vector determined at time t_{k+1} are taken as initial data. If this difference $\Delta\boldsymbol{Y}^{(m)}(t_{k+1})$ is greater than $\varepsilon_{\boldsymbol{Y}}$, the improved value of control vector $\boldsymbol{S}^{(m+1)}(t_k)$ is calculated. For this purpose Newton's method is applied. According to this method, the expression for $\boldsymbol{S}^{(m+1)}(t_k)$ is as follows

$$\boldsymbol{S}^{(m+1)}(t_k) = \boldsymbol{S}^{(m)}(t_k) + \mathbf{J}^{-1}\Delta\boldsymbol{Y}^{(m)}(t_{k+1}) \tag{3.9}$$

where $\mathbf{J}$ is the Jakobian. Its elements are determined by the formula

$$J_{ij}(t_k) = \frac{\partial[\Delta Y_i^{(m)}(t_{k+1})]}{\partial S_j^{(m)}(t_k)} = \frac{\partial Y_i^{(m)}(t_{k+1})}{\partial S_j^{(m)}(t_k)} \tag{3.10}$$

Because the considered problem is solved numerically, then the following differential scheme is applied

$$J_{ij}(t_k) = \frac{Y_i^{(m)}[t_{k+1}, S_j^{(m)}(t_k) + \delta S_j^{(m)}] - Y_i^{(m)}[t_{k+1}, S_j^{(m)}(t_k) - \delta S_j^{(m)}]}{2\delta S_j^{(m)}} \tag{3.11}$$

The expression (3.9) is a result of the following procedure:

- The output vector $\boldsymbol{Y}^{(m)}(t_{k+1})$ is calculated at the time point t_{k+1} at mth iteration. It depends on the flight parameters vector $\boldsymbol{X}(t_k)$ and the control vector $\boldsymbol{S}^{(m)}(t_k)$, which are determined at the previous time point t_k.

  If the calculations are performed again for a modified value of the control vector

  $$\boldsymbol{S}^{(m+1)}(t_k) = \boldsymbol{S}^{(m)}(t_k) + \Delta\boldsymbol{S}^{(m)}(t_k) \tag{3.12}$$

  one can obtain a new value of the output vector $\boldsymbol{Y}^{(m+1)}(t_{k+1})$ for the $(m+1)$th iteration.

  Making use of the Taylor series and taking into account only linear part of the expansion in series, one can assume that

  $$\boldsymbol{Y}^{(m+1)}(t_k) = \boldsymbol{Y}^{(m)}(t_{k+1}) + \mathbf{J}\Delta\boldsymbol{S}^{(m)}(t_k) \tag{3.13}$$

  where Jacobian elements are determined by relations (3.10) and (3.11). Using relation (3.13), after elementary transformations, one can obtain formula (3.9), which allows to calculate the control vector at time t_k for the $(m+1)$th iteration $\boldsymbol{S}^{(m+1)}(t_k)$. It is assumed that the calculated value of the output vector $\boldsymbol{Y}^{(m+1)}(t_{k+1})$ has to be equal to the determined value $\boldsymbol{Y}^{(m+1)}(t_{k+1}) = \boldsymbol{Y}_z(t_{k+1})$. It is taken into account in relation (3.8).

4. Simulation of selected aircraft spatial manoeuvres

To illustrate efficiency of the applied inverse method of simulation, some results of numerical calculation for selected spatial manoeuvres are shown below. To verify the numerical algorithm, time courses of different flight parameters have been taken as the constrains. But for all cases, the following rule was required: among four selected parameters, which were the constraints, two were the longitudinal parameters (two from V, α, Q, Θ for an aeroplane or two from U, W, Q, Θ for a helicopter), and two other were connected with a lateral motion (two from β, P, R, Φ, Ψ for an aeroplane or two from V, P, R, Φ, Ψ for a helicopter). Selection of these parameters has been performed in order to complete the description of a concrete aircraft manoeuvre. Calculations have been done for aeroplanes MiG-29 and TS-11 *Iskra*, and for Polish helicopter *Sokol*. Several manoeuvres have been simulated. In this paper, one aeroplane's manoeuvre and one helicopter's manoeuvre are presented.

4.1. Roll manoeuvre

Roll is a typical manoeuvre of an aeroplane. It was supposed that the roll was performed by rotation about the longitudinal axis of the fuselage Ox_k. Steady-state flight was assumed as the initial condition. It was executed with velocity $V = 200\,\mathrm{m/s}$. Angle of incidence was equal to $\alpha_0 = 1.61^\circ$ and thrust was equal to $T_c = 7329\,\mathrm{N}$. An assumption was made that the velocity and the pitch angle of aeroplane were stable

$$\begin{aligned} V(t) &= 200\mathrm{m/s} = \text{const} \\ \Theta(t) &= \Theta_0 = \alpha_0 = 1.61^\circ = \text{const} \end{aligned} \tag{4.1}$$

Two next constraints connected with lateral motion were as follows:

- the yaw angle was equal to zero $\Psi(t) = 0 = \text{const}$
- changes of the roll angle Φ were determined by the following formula

$$\Phi(t) = \begin{cases} 0 & \text{for} \quad t < t_0 \\ \dfrac{2\pi}{16}\left[\cos\left(3\pi\dfrac{t-t_0}{T}\right) - 9\cos\left(\pi\dfrac{t-t_0}{T}\right) + 8\right] & \text{for} \quad t_0 \leqslant t \leqslant t_0 + T \\ 2\pi & \text{for} \quad t > T \end{cases} \tag{4.2}$$

In the presented simulation, the beginning of the roll was at the 2nd second of flight and it was completed at the 7th second. It means that $t_0 = 2\,\mathrm{s}$,

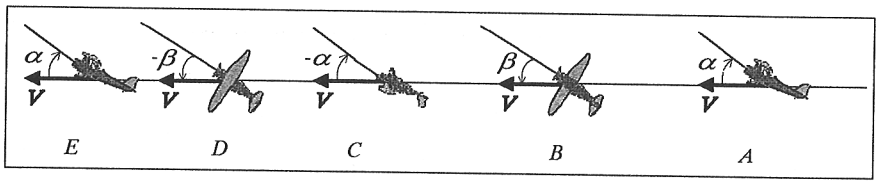

Fig. 1. Roll manoeuvre

$T = 5$ s. Time courses of some selected parameters $\Phi(t)$, $\alpha(t)$, $\beta(t)$, are shown in Fig.2 ÷ Fig.4 and three calculated control parameters $\delta_H(t)$, $\delta_L(t)$, $\delta_V(t)$ are presented in Fig.5 ÷ Fig.7 (engine thrust $T_c(t)$ is not presented). Because constrains (4.1) and (4.2) are strictly satisfied, they are not presented except for the roll angle, which is shown in Fig.2. From this figure one can see that constraints of the motion are satisfied exactly. It is shown that during the roll manoeuvre, the angle of incidence and the sideslip angle change. For performing this manoeuvre it is necessary to control the aeroplane using all the control devices.

4.2. Deceleration with bob up to hover

Deceleration with bob up to hover is one of the Nap-of-the-Earth manoeuvres. It is characterised by a rapid velocity deceleration with vertical translation and the following staying in a hover. According to data from the Flight Data Recorder (FDR), the following constraints were taken into account:

— rolling and yawing angular velocities were equal to zero

$$P(t) = R(t) = 0 \tag{4.3}$$

— the time history of the desired vertical position was given as

$$z_g(t) = \begin{cases} 0 & \text{for} \quad t < t_{mH} \ \wedge \ t \geqslant t_{mH} + T_{dH} \\ \dfrac{-H_{\max}}{16}\left[\cos\left(3\pi\dfrac{t - t_{mH}}{T_{dH}}\right) - 9\cos\left(\pi\dfrac{t - t_{mH}}{T_{dH}}\right) + 8\right] & \text{for} \quad t_{mH} \leqslant t \leqslant t_{mH} + T_{dH} \end{cases} \tag{4.4}$$

where $t_{mH} = 0$ s, $T_{dH} = 5$ s, $H_{\max} = -16$ m/s.

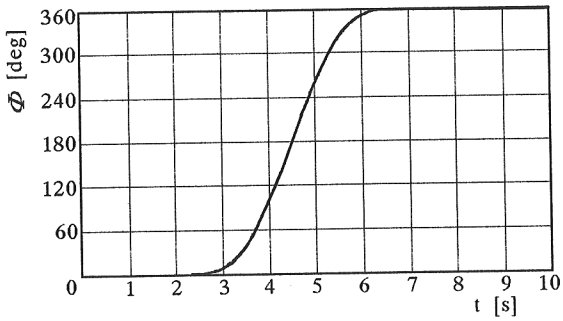

Fig. 2. Roll angle $\Phi(t)$

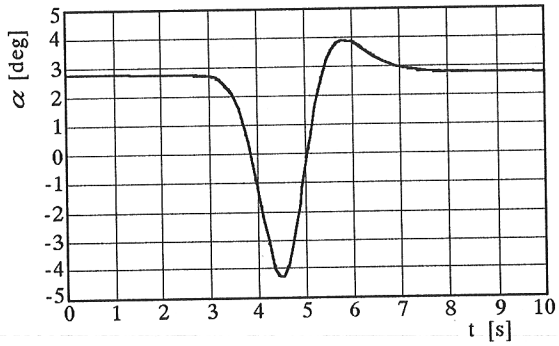

Fig. 3. Angle of attack $\alpha(t)$

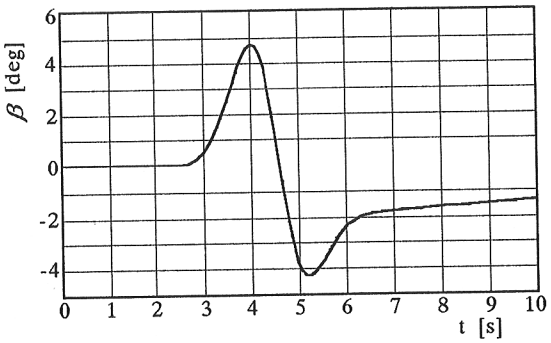

Fig. 4. Sidestep angle $\beta(t)$

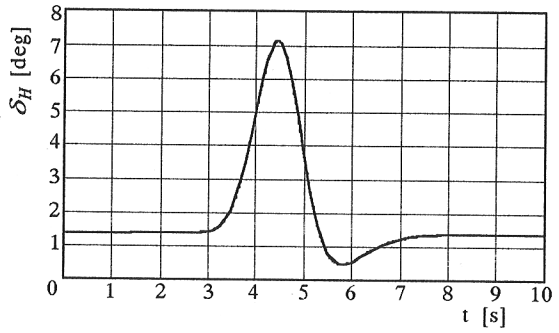

Fig. 5. Stabilator deflection $\delta_H(t)$

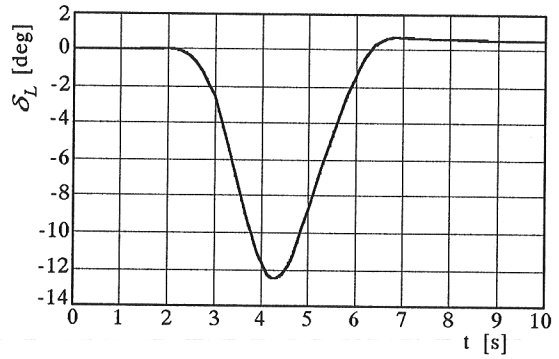

Fig. 6. Aileron deflection $\delta_L(t)$

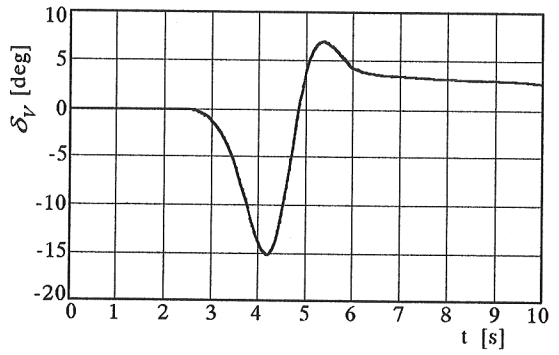

Fig. 7. Rudder deflection $\delta_V(t)$

— the pitching angular velocity changed as follows

$$Q(t) = \begin{cases} 0 & \text{for } t < t_{m1Q} \ \wedge \ t > t_{m6Q} + T_{d6Q} \\ \dfrac{Q_A}{16}\square_1 & \text{for } t_{m1Q} \leqslant t < t_{m1Q} + T_{d1Q} \\ Q_A & \text{for } t_{m1Q} + T_{d1Q} \leqslant t < t_{m2Q} \\ Q_A - \dfrac{Q_A - Q_B}{16}\square_2 & \text{for } t_{m2Q} \leqslant t < t_{m2Q} + T_{d2Q} \\ Q_B & \text{for } t_{m2Q} + T_{d2Q} \leqslant t < t_{m3Q} \\ Q_B + \dfrac{Q_B - Q_C}{16}\square_3 & \text{for } t_{m3Q} \leqslant t < t_{m3Q} + T_{d3Q} \\ Q_C & \text{for } t_{m3Q} + T_{d3Q} \leqslant t < t_{m4Q} \\ Q_C - \dfrac{Q_C - Q_D}{16}\square_4 & \text{for } t_{m4Q} \leqslant t < t_{m4Q} + T_{d4Q} \\ Q_D & \text{for } t_{m4Q} + T_{d4Q} \leqslant t < t_{m5Q} \\ Q_C - \dfrac{Q_C - Q_E}{16}\square_5 & \text{for } t_{m5Q} \leqslant t < t_{m5Q} + T_{d5Q} \\ Q_E & \text{for } t_{m5Q} + T_{d5Q} \leqslant t < t_{m6Q} \\ Q_E - \dfrac{Q_E}{16}\square_6 & \text{for } t_{m6Q} \leqslant t < t_{m6Q} + T_{d6Q} \end{cases} \tag{4.5}$$

where

$$\square_i = \left[\cos\left(3\pi\frac{t - t_{miQ}}{T_{diQ}}\right) - 9\cos\left(\pi\frac{t - t_{miQ}}{T_{diQ}}\right) + 8\right] \qquad i = 1, 2, ..., 6$$

and

$t_{m1Q} = 0$ s $\quad T_{d1Q} = 1.6$ s $\quad t_{m4Q} = 4.5$ s $\quad T_{d4Q} = 2.5$ s

$t_{m2Q} = 1.6$ s $\quad T_{d2Q} = 1.4$ s $\quad t_{m5Q} = 7$ s $\quad T_{d5Q} = 1.6$ s

$t_{m3Q} = 3$ s $\quad T_{d3Q} = 1.5$ s $\quad t_{m6Q} = 8.6$ s $\quad T_{d6Q} = 1.4$ s

$Q_A = 31.58° \text{ s}^{-1} \quad Q_B = -10° \text{ s}^{-1} \quad Q_C = 0° \text{ s}^{-1}$

$Q_D = -20.22° \text{ s}^{-1} \quad Q_E = 6.25° \text{ s}^{-1}$

The steady state flight at $V = 25$ m/s was the initial condition.

Fig.8 ÷ Fig.13 present some results of numerical simulations of bob-up-to-hover manoeuvre. For comparison, the data from the FDR is also depicted. One can observe that the recorded and calculated parameters are in good agreement. Differences are also observed. The observed differences are due to simplifications of the mathematical model of a helicopter and due to inherent features of the analytical method of determination of the constraints.

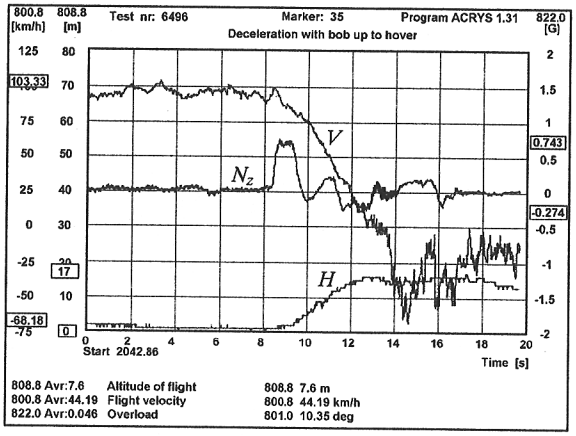

Fig. 8. Recorded flight velocity, altitude and overload

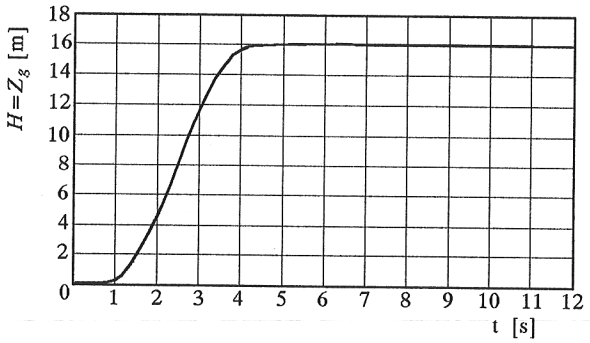

Fig. 9. Altitude of flight – simulation

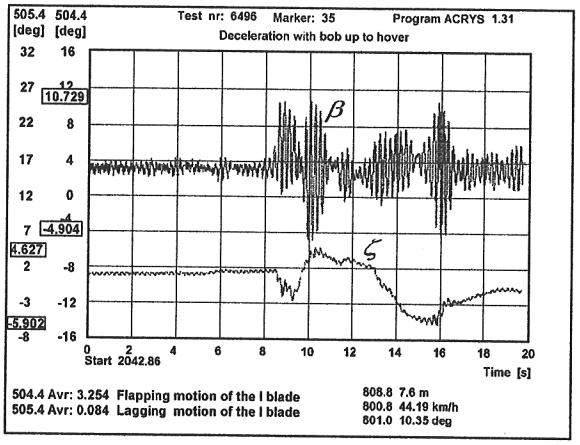

Fig. 10. Recorded flapping of blade

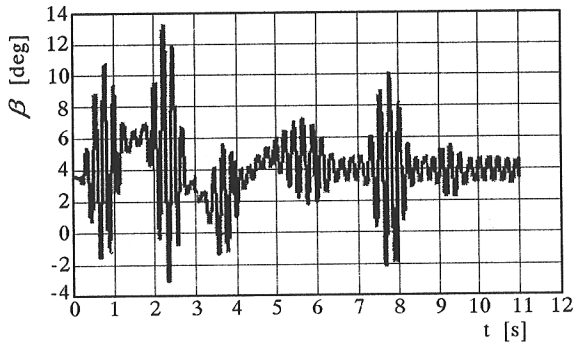

Fig. 11. Flapping of blade – simulation

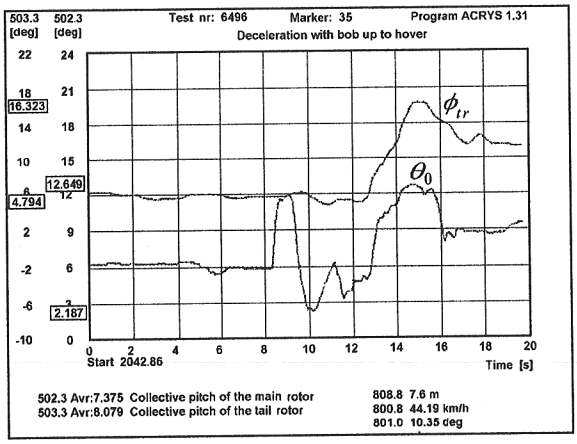

Fig. 12. Recorded collective pitch angles

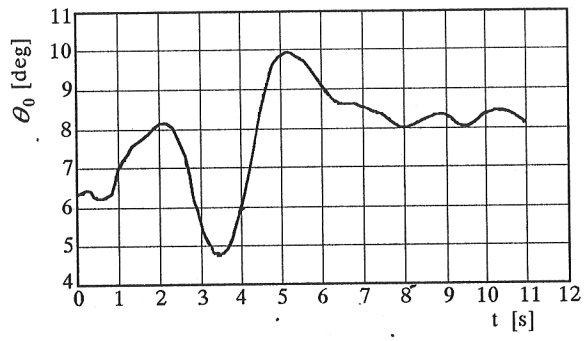

Fig. 13. Collective pitch of the main rotor – simulation

5. Conclusions

A relatively simple numerical methodology was employed for determining the controls, which are necessary to perform a constrained flight, both for an aeroplane and for a helicopter. On the basis of the performed calculations, the following conclusions can be formulated:

- A very high accuracy of determining the output vector is required.
- This accuracy is strictly limited by errors of numerical rounding.
- High gradients or discontinuities of constraints are causes of the determined controls broadening.
- The method was not succeeded in determining control signals on the basis of trajectory of flight.

Acknowledgement

This works is partially supported by the State Committee for Scientific Research under Grants No. 9 T12C 078 14 and 9 T12C 047 13.

References

1. BLAJER W., 1994a, *Metoda projekcyjna – teoria i zastosowania w badaniu nieswobodnych układów mechanicznych*, Wyższa Szkoła Inżynierska im. Kazimierza Puławskiego, Radom
2. BLAJER W., 1994b, Uwagi o realizacji programowego ruchu samolotu po założonej trajektorii, *Mechanika w Lotnictwie, ML-VI'94*, ZG PTMTS
3. BLAJER W., PARCZEWSKI J., 1987, Model matematyczny wyznaczania funkcji sterowania samolotem w pętli, *Mechanika Teoretyczna i Stosowana*, 1/2, **25**
4. BLAJER W., PARCZEWSKI J., 1991, Modelowanie figur akrobacji lotniczej jako programowego lotu samolotu, *Mechanika Teoretyczna i Stosowana*, 2, **29**
5. GALIULLIN A.S., 1986, *Metody resheniya obratnykh zadach dinamiki*, Izd. Nauka, Moskwa
6. HESS R., GAO C., WANG S., 1991, Generalized Technique for Inverse Simulation Applied to Aircraft Flight Control, *Journal of Guidance, Control and Dynamics*, **14**, 5

7. HESS R.A., GAO C., 1993, A Generalized Algorithm for Inverse Simulation Applied to Helicopter Maneuvering Flight, *Journal of the American Helicopter Society*, **38**, 4

8. RUTHERFORD S., THOMSON D., 1996a, Helicopter Inverse Simulation Incorporating an Individual Blade Rotor Model, *Proceedings of 20-th ICAS Congress*, Sorrento

9. RUTHERFORD S., THOMSON D., 1996b, Improved Methodology for Inverse Simulation, *Aeronautical Journal*, **100**, 933

10. THOMSON D.G., BRADLEY R., 1990, Development and Validation of an Algorithm for Helicopter Inverse Simulations, *Vertica*, **14**, 2

11. TOMCZYK A., 1996, Kształtowanie właściwości pilotażowych samolotu poprzez zastosowanie nieliniowej dynamiki odwrotnej i dekompozycji zadania sterowania, *Mechanika w Lotnictwie, ML-VII'96*, ZG PTMTS

Modyfikacja numeryczna symulacji odwrotnej manewrów statków powietrznych

Streszczenie

W pracy przedstawiono metodę numerycznej symulacji manewrów przestrzennych statków powietrznych. Metoda ta oparta jest na rozwiązaniu zagadnienia odwrotnego. Bazuje ona na linearyzacji problemu wokół bieżącego położenia w przestrzeni stanów. Pokazano wyniki symulacji "beczki" wykonywanej przez samolot oraz "wyskoku do zawisu" realizowanego przez śmigłowiec. W drugim przypadku wyniki symulacji porównano z zapisami parametrów lotu zarejestrowanymi w czasie wykonywania takiego manewru.

Manuscript received March 28, 2000; accepted for print June 6, 2000